Accumulation and Changes in Composition of Collagens in Subcutaneous Adipose Tissue After Bariatric Surgery

Yuejun Liu, Judith Aron-Wisnewsky, Geneviève Marcelin, Laurent Genser, Gilles Le Naour, Adriana Torcivia, Brigitte Bauvois, Sandrine Bouchet, Véronique Pelloux, Magali Sasso, et al.

Accumulation and Changes in Composition of Collagens in Subcutaneous Adipose Tissue Following Bariatric Surgery

Yuejun Liu[1,2,3,4], Judith Aron-Wisnewsky[1,2,3,5], Geneviève Marcelin[1,2,3], Laurent Genser[1,2,3,6], Gilles Le Naour[7], Adriana Torcivia[6], Brigitte Bauvois[8], Sandrine Bouchet[8], Véronique Pelloux[1,2,3], Magali Sasso[4], Véronique Miette[4], Joan Tordjman[1,2,3], Karine Clément[1,2,3,5]

1. Institute of Cardiometabolism and Nutrition, ICAN, F-75013, Paris, France

2. INSERM, UMRS 1166, Nutriomic team 6, Paris, F-75013 France

3. Sorbonne Universités, UPMC Université Paris 06, UMRS 1166, F-75005, Paris, France

4. Echosens Research Department, Paris, France

5. Assistance Publique-Hôpitaux de Paris (AP-HP), Pitié-Salpêtrière Hospital, Nutrition Department, Paris, F-75013 France

6. Assistance Publique-Hôpitaux de Paris (AP-HP), Pitié-Salpêtrière Hospital, Department of Digestive and Hepato-Pancreato-Biliary Surgery, Paris, F-75013 France

7. Assistance Publique-Hôpitaux de Paris (AP-HP), Pitié-Salpêtrière Hospital, Department of Pathology, UIMAP, UPMC Université Paris 06, Paris, F-75013 France

8. Centre de Recherche des Cordeliers, INSERM UMRS 1138, Sorbonne Universités UPMC Paris 06, Université Paris Descartes Sorbonne Paris Cité, F-75006 Paris, France

***Abbreviated title*:** Adipose Tissue Remodeling during Weight Loss

Key words: adipose tissue remodeling; collagen accumulation; fibrosis; cross-linking; weight loss

Word counts (≤3600): **4230**

Number of figures and tables (≤6): 6

Corresponding author and the person to whom reprint requests should be addressed:

Karine Clément, MD, PhD

Address: E3M building – 6th floor, 46-83 Boulevard de l'Hôpital, 75013, Paris.

Tel: 33(0) 1 4217 7928.

E-mail: karine.clement@psl.aphp.fr

***Funding*:** This work was supported by several clinical research contracts (Assistance Publique-Hôpitaux de Paris CRC FIBROTA to JAW and KC and PHRC 0702 to KC) and funding from the Fondation pour la Recherche Médicale (FRM DEQ20120323701), the National Agency of Research (ANR, Adipofib), the national program "Investissements d'Avenir" with the reference ANR-10-IAHU-05 and CIFRE N° 2012/1180.

Disclosure summary: Y.L. received support from Echosens for her PhD program, M.S. And V.M are employees from Echosens. All other authors including J.AW., G.M., L.G., G.L.N, A.T., B.B., S.B., J.T., K.C. declare no conflict of interest.

Clinical Trial Registration Number: ClinicalTrials.gov NCT01655017

ABSTRACT (249 words)

Context: Extracellular matrix (ECM) in subcutaneous adipose tissue (scAT) undergoes pathological remodeling during obesity. However, its evolution during weight loss remains poorly explored.

Objective: To study histological, transcriptomic and physical characteristics of scAT ECM remodeling during the first year of bariatric surgery (BS)-induced weight loss and their relationships with metabolic and bioclinical improvements.

Patients and Main measures: 118 morbidly obese candidates for BS were recruited and followed during one-year post-BS. ScAT surgical biopsy and needle aspiration, as well as scAT stiffness measurement were performed in three sub-groups before and post-BS. 14 non-obese non-diabetic subjects served as controls.

Results: Significantly increased picrosirius-red stained collagen accumulation in scAT post-BS was observed along with fat mass loss, despite metabolic and inflammatory improvements and undetectable changes of scAT stiffness. Collagen accumulation positively associated with M2-macrophages ($CD163^+$ cells) before BS but negatively after. Expression levels of genes encoding ECM components (e.g. COL3A1, COL6A1, COL6A2, ELN), cross-linking enzymes (e.g. LOX, LOXL4, TGM), metalloproteinases and their inhibitors were modified one-year post-BS. LOX expression and protein were significantly decreased, and associated with decreased fat mass, as well as other cross-linking enzymes. Although total collagen I and VI staining decreased one-year post-BS, we found increased degraded collagen I and III in scAT, suggesting increased degradation.

Conclusions: After BS-induced weight loss and related metabolic improvements, scAT displays major collagen remodeling with an increased picrosirius-red staining that relates to increased collagen degradation and importantly decreased cross-linking. These features are in agreement with adequate ECM adaptation during fat mass loss.

The extracellular matrix (ECM) in subcutaneous adipose tissue (scAT) undergoes substantial pathological remodeling during obesity. ECM accumulation, usually called fibrosis, is defined as an excessive deposition of ECM components (mainly cross-linked collagens) and impaired degradation (1). ECM accumulation is important in the regenerative step where it replaces damaged cells. However, if the damage persists, excessive ECM deposition harms tissue homeostasis and function (2). In obesity, scAT ECM accumulation reduces tissue plasticity and results in adipocyte dysfunction, ectopic fat storage, and metabolic disorders (1). Studies have shown the detrimental consequences of ECM accumulation in obesity and their associations with comorbidities. In mice, genetic ablation of MT1-MMP, a membrane anchored metalloproteinase degrading collagen I, leads to increased peri-adipocyte fibrosis and severe metabolic complications such as hepatic steatosis (3). Likewise, Collagen VI accumulation in obesity is associated with insulin resistance (4,5). By contrast, the absence of collagen VI in high-fat diet or *ob/ob* mice results in uninhibited adipocyte expansion and associates with metabolic and inflammatory improvements (6). In obese subjects, scAT fibrosis is increased (7,8). Moreover, higher scAT fibrosis at baseline is associated with lower weight loss one year post-bariatric surgery (BS) (7,9). In addition, scAT pericellular fibrosis is associated with liver fibrosis, suggesting that obesity is a profibrotic condition (9). Finally, the pericardial fat secretome was also found to promote myocardial fibrosis (10). Overall, these studies underline the potential deleterious effects of obesity-induced scAT ECM accumulation.

Mechanistically, scAT fibrosis leads to adipocyte dysfunction and fibro-inflammation through a mechano-transduction pathway (11). Lysyl oxidase (LOX), an important matrix fibers' cross-linking enzyme, contributes to tissue mechanical properties (12). In AT, LOX expression is up-regulated in high-fat diet or *ob/ob* mice. By contrast, inhibition of LOX activity leads to improved metabolism and inflammation (13). In obese subjects, scAT LOX expression is also increased (11). ScAT stiffness, measured non-invasively by transient elastography, associates with picrosirius-red stained scAT fibrosis and altered glucose homeostasis (9).

ECM turnover, a crucial process during excess ECM accumulation, is predominately regulated by the balance between matrix metalloproteinases (MMPs) and their endogenous tissue inhibitor of metalloproteinases (TIMPs). In obesity, a new relationship between MMPs and TIMPs is established and enables tissue remodeling. Enzymes (e.g. MMP-3, -9, -11, -12, -13, -16, and -24) are expressed at low level in scAT, but are rapidly up-regulated during obesity, which eventually favors scAT expansion (1). Weight loss represents another condition that induces scAT remodeling, exhibiting by changes in expression of many ECM genes soon after BS (8,14).

Some studies have shown increased ECM deposition, e.g. up-regulated collagens, particularly COL6A3, after major weight loss in a long-term (14,15). However, most of these studies focused on selected collagens at expression levels and did not explore the overall ECM characteristics. Furthermore, no study has yet evaluated the links between scAT ECM remodeling, stiffness, and modifications in cross-linking enzymes, and improved metabolic parameters after weight loss.

Herein, we examined fibrillar collagen accumulation, synthesis, and degradation as well as cross-linking enzymes, macrophage infiltration and scAT stiffness during the first year post-BS. We also analyzed relationships between ECM properties and metabolic and inflammatory parameters improvements observed post-BS.

Materials and Methods

Study Population

A total of 118 morbidly obese candidates for BS who met the recruitment criteria as described (7) were enrolled at the Institute of Cardiometabolism and Nutrition (ICAN), Nutrition Department and operated in the Department of Surgery, Pitié-Salpêtrière Hospital (Paris). **Due to the difficulties to obtain large amount of scAT surgical biopsy sample in every subject during the follow-up and the number of experiments to perform on these samples, we divided our overall cohort into 3 groups according to the different scAT measurements that were realized** (study flowchart see Figure 1). However, subjects were part of the same prospective cohort and baseline (T0) characteristics were not significantly different (Table 1).

Group1 subjects (**n=52**, **age 40.1±10.2yr, female n=37 (71%), BS procedures: gastric banding (GB) n=8 (15%), sleeve gastrectomy (SG) n=16 (31%), Roux-en-Y gastric bypass (RYGB) n=28 (54%)**) accepted surgical scAT biopsy before (T0) and 3 months (T3) and 12 months (T12) post-BS. Surgical biopsy was performed under local anesthesia in peri-umbilical area as described (15,16). The collected scAT samples were used for explant experiments and histological analysis.

Group2 (n=35, **age 38.0±10.0yr, female n=24 (69%), BS procedures: GB n=3 (8%), SG n=16 (46%), RYGB n=16 (46%)**) underwent at T0, T3, and T12 scAT stiffness measurement (see below). A sub-group of 14 non-diabetic women from Group2 underwent scAT needle aspiration for RT-PCR analysis. Notably, 11 individuals with stiffness measurement were also part of Group1.

Group3 (n=42, **age 42.9±10.5yr, female n=42 (100%), BS procedures: RYGB n=42 (100%)**) underwent scAT needle aspiration at T0 and T12 for microarray analysis.

14 non-obese non-diabetic subjects (age=41.6±14.1yr, female 29%, BMI=23.2±3.3 kg/m^2), who had elective abdominal programmed surgery without inflammatory diseases as described (7), were recruited as a control group. Perioperative scAT biopsy samples were collected in the same location as in obese subjects. Ethical approval was obtained from the Research Ethics Committee of Pitié-Salpêtrière Hospital (CPP Ile de France). Informed written consent was obtained from all subjects.

Clinical, Anthropological and Biological Parameters

Body composition was evaluated by whole body fan-beam dual energy X-ray absorptiometry (DXA) scan (Hologic Discovery W, Bedford, MA) as described (9). Blood samples were collected after 12-hour overnight fast at T0, T3, and T12. Clinical variables were measured as described (7). Pancreatic beta-cell function (insulin secretion), insulin sensitivity and resistance were estimated using Homeostatic Model Assessment – Continuous Infusion Glucose Model Assessment (HOMA-CIGMA) (17) .

Measurement of scAT Shear Wave Speed by Transient Elastography

A new non-invasive medical device based on transient elastography (18), Adiposcan^{TM} (Echosens, Paris, France), was developed to measure scAT shear wave speed (SWS) associated with scAT stiffness (9,19). ScAT stiffness was measured by the same operator in obese subjects (Group2) in the right peri-umbilical region at T0, T3 and T12.

Transcriptomic Experiments

ScAT samples obtained by needle aspiration at T0 and T12 (Group3) were stored at -80°C for microarray analysis. Total RNA extraction, amplification, hybridization and raw data analysis were performed as described (20). The complete dataset is published in the NCBI Omnibus (http://www.ncbi.nlm.nih.gov/geo/) through the series accession number GSE72158.

RT-PCR for selected genes was performed as described (20), using total RNA extracted from scAT needle aspiration in 14 non-diabetic obese women (Group2) at T0, T3 and T12.

Tissue Preparation and Histological Analysis of scAT

A piece of surgical biopsy sample was fixed and embedded in paraffin and sliced into 5µm-thick sections. Collagen was stained with picrosirius-red (mainly collagen I and III) and analyzed using Calopix software (Tribvn, Châtillon, France) in 36 subjects (Group1) at T0, T3 and T12 as described (9). Total collagen accumulation represents the

ratio of the stained fibrous area to the total tissue surface. Pericellular collagen accumulation (i.e. collagen surrounding adipocytes) represents the ratio of the stained area in 10 random fields avoiding fibrosis bundles. Adipocyte diameters were evaluated in the same 10 fields. Pericellular collagen accumulation was adjusted by adipocyte size to eliminate the effects of different adipocyte sizes in measure fields. Collagen I and VI, degraded collagen I, LOX and macrophages were detected by immunohistochemistry **(IHC)** using specific antibodies (Supplemental Table 1). Total macrophages were defined as $CD68^+$ cells and M2-macrophages as $CD163^+$ cells. Their results are expressed as the number of $CD68^+$ or $CD163^+$ cells related to 100 adipocytes (21). Collagen and elastin structures were analyzed using confocal microscopy and second-harmonic generation (SHG) microscopy on another piece of fixed scAT sample in 3 random obese subjects (Group1) as described (11).

ScAT Explant *in vitro*

Piece of surgical biopsy samples (Group1) was placed in a culture medium enriched in endothelial cell basal medium (Promocell, Heildelberg, Germany), supplemented with 1% albumin free fatty acids (PAA Laboratoires, Velizy-Villacoublay, France) and antibiotics. After 24-hour incubation at 37°C, scAT explant secretion media were collected and frozen at -80°C for ELISA and zymography. The explant secretion was normalized to AT weight according to the ratio of 1mL of culture medium for 0.1g scAT.

Protein Determination in scAT Explant

The concentrations of collagen III formation marker, N-proteases cleaved N-terminal propeptides of collagen III (PRO-C3), and degradation marker, MMP-9-generated neoepitope fragments of collagen III (C3M), in scAT explants were evaluated using two competitive ELISA kits developed by Nordic Bioscience A/S (Herlev, Denmark) (22). The protein profiles of proMMP-2 and proMMP-9 were analyzed by zymography as described (23).

Statistical Analyses

Data are expressed as mean ± SD, categorical variables as numbers and percentages, and values in graphs as mean ± SEM. Categorical data were analyzed using Fisher's exact test. For continuous data, repeated one-way ANOVA was used to compare more than two groups and Holm-Sidak's parametric multiple comparison for post-hoc analysis; student's t-test was used to compare two groups. **K-means for longitudinal data (KmL) was used to cluster scAT stiffness trajectories.** For small sample size (i.e. $n<30$), data were first transformed by natural logarithm if they did not follow a Gaussian distribution. Two-tailed p-values were considered significant below

0.05. All analyses were conducted using R software version 3.0.3 (http://www.r- project.org) and GraphPad Prism 6.0.

Results

Increased Collagen Deposition in scAT during BS-induced Weight Loss

Using picrosirius-red staining, scAT collagen was quantified in **36-paired** obese subjects (Group1) at **baseline (T0) and during the follow-up (T3 and T12)**. No significant difference **in collagen accumulation** was found among **the** different BS procedures at baseline (Supplemental Table2). More abundant and thicker bundles of collagen fibers traversing the scAT were observed at T3 and T12 (Figure 2A, B, C). Several parenchymal areas were filled with less well-organized collagen in post-operative tissues (Figure 2C, enlarged image). A significant increase in the average of total and pericellular collagen was observed at T3 and T12 (Figure 2D). As expected, adipocyte size significantly decreased post-BS (Figure 2E), but this reduction was not correlated with collagen accumulation. Moreover, the increase in pericellular collagen remained significant after adjustment for adipocyte size reduction. Importantly, the fat mass reduction was negatively correlated with pericellular collagen accumulation ($r=-0.40$, $p<0.05$). No other associations were observed between collagen accumulation and metabolic or inflammatory variables except for systemic HDL-cholesterol (Supplemental Table3). Importantly, the results hold true in sub group analysis in each different bariatric surgery technic data not shown).

Undetectable Changes in Tissue Stiffness despite Increased scAT Collagen Accumulation in scAT

Since we **previously** showed that collagen accumulation was associated with scAT rigidity **and metabolic alterations** in obesity (9), we **next** aimed to investigate scAT stiffness changes post-BS using Adiposcan™ at T0, T3 and T12 (Group2). **To our surprise, d**espite increased collagen accumulation, no significant change in **average** SWS was detected at T3 and T12 compared to T0 (T0: 0.90±0.29m/s, T3: 0.88±0.28m/s, T12: 0.93±0.43m/s, $p=0.58$, Figure 2F). **Using K-means for longitudinal data (KmL) to cluster scAT stiffness individual trajectories, we observed 2 major clusters (A and B) of stiffness changes that suggest different profiles of tissue response post-BS (Figure 2G). Cluster A (n=24) had significant lower stiffness than Cluster B (n=12) at T0 (Cluster A 0.78±0.15m/s vs Cluster B 1.17±0.35m/s, Wilcoxon test $p<0.05$) and T12 (Cluster A 0.68±0.18m/s vs Cluster B 1.47±0.32m/s, Wilcoxon test $p<0.05$), while Cluster B displayed a V-shape profile with an initial decrease and a subsequent increase. However, we did not observe significant bioclinical differences at any time points that could possibly explain these trajectories (Supplemental Table 4). The absence of significant change in average scAT SWS suggested that stiffness was not increased after surgery**

despite increased picrosirius-red stained collagen. Therefore, this increase in collagen accumulation could be considered as adaptive ECM remodeling requiring further investigation.

M2-Macrophages Associate with Collagen Accumulation in scAT

M2 cells, alternatively activated macrophages, are implicated in the resolution phase of inflammation and tissue remodeling (24). **Using IHC,** M2 cells (i.e.$CD163^+$ cells) and total macrophages (i.e.$CD68^+$ cells) in scAT were quantified in 15 obese subjects from Group1 at T0 and T12. The $CD163^+/CD68^+$ ratio increased between T0 and T12 (0.38±0.20 vs. 0.78±0.58, $p<0.01$, Figure 3A), in agreement with a switch toward M2-macrophages during weight loss and their role in tissue remodeling. At T0, a strong positive association between $CD163^+$ cells and pericellular collagen accumulation was observed ($r=0.76$, $p<0.01$, Figure 3D left panel). Although the number of $CD163^+$ cells moderately increased at T12 (6±3% vs. 9±4%, $p=0.04$, Figure 3B), a negative association between $CD163^+$ count and pericellular collagen accumulation was found ($r=-0.65$, $p=0.02$, Figure 3D right panel). By contrast, the number of $CD68^+$ cells decreased between T0 and T12 (17±8% vs. 14±7%, $p=0.04$, Figures 3C), but was not associated with collagen deposition at T0 or T12.

Major ECM Remodeling at Transcriptomic Level after Weight Loss

As BS-induced weight loss is accompanied by increased collagen deposition without detectable one-year change in SWS, we next characterized transcriptomic signatures of scAT at T0 and T12 in 42 women (Group3). Using a 5% false-discovery rate, we detected 4236 up- and 2989 down-regulated genes (functional annotations see Supplemental Figure 1). We focused our analysis on genes encoding proteins involved in ECM structural components, profibrotic proteins, remodeling, and mechanotransduction. We found differential patterns of gene changes (Figure 4A). Particularly, genes encoding collagen III (COL3A1), collagen VI (COL6A1, COL6A2), and elastin (ELN) were significantly down-regulated, while collagen I (COL1A1) was unchanged. Collagen VI alpha 3 chain (COL6A3) was modestly up-regulated. Connective tissue growth factor (CTGF) and secreted phosphoprotein 1 (osteopontin, SPP1) were significantly down-regulated. MMP-9, TIMP1, TIMP2, and TIMP4 were also significantly modified. Importantly, some genes previously shown to be stimulated by mechanical stress (11), such as YAP, TEAD2, TEAD3, TEAD4, were not modified after weight loss ($p>0.05$).

During collagen biosynthesis, major post-translational modifications take place and are mediated by important enzymes and chaperones. We found that the expression levels of most of these molecules were decreased at T12 (Figure 4B). Finally, we observed a significant down-regulation of genes encoding cross-linking enzymes such as LOX, lysyl oxidase-like 4 (LOXL4), transglutaminase1 (TGM1), procollagen-lysine, 2-oxoglutarate 5-dioxygenase 2 and 3 (PLOD2 and PLOD3), suggesting that matrix fibers' cross-linking was decreased post-BS (Figure 4A). These transcriptomic analyses confirm the strong remodeling of scAT following BS and show major transcriptomic modifications of enzymes involved in collagen biosynthesis, cross-linking and degradation.

Decreased Cross-linking of Matrix Fibers during Weight Loss Associates with Improved Metabolic Phenotype

We next explored cross-linking enzymes and their associations with metabolic phenotypes. We confirmed microarray data by RT-PCR and observed that LOX gene expression was significantly down-regulated at T3 and T12 (Group2) (Figure 5A). This was substantiated by decreased LOX protein staining surrounding adipocytes at T3 and T12 (Figure 5B) **using IHC**. By confocal microscopy and SHG in fixed scAT samples in 3 random obese subjects (Group1), we found a trend towards reduced collagen and elastin intensity at T3 (Supplemental Figure 2). Elastin protein at T3 had more twisted structures (Figure 5C), suggesting that scAT might become less rigid after weight loss.

We next examined the relationships between one-year changes in cross-linking enzyme expression and that of clinical variables (i.e.T12-T0 variation) in Group3 (Figure 5D). The reduction of LOX gene expression was positively associated with the reduction of BMI, fat mass (kg), adipocyte volume, serum leptin and orosomucoid. Variation of LOXL1 was also associated with BMI, fat mass (kg), leptin, total- and HDL-cholesterol. Our gene expression results suggest that decreased post-BS cross-linked scAT matrix fibers in link with improved weight loss.

Increased Collagen Degradation during BS-induced Weight Loss

Our team (7) and others (4) have shown that collagen I and III are more frequently observed in fibrous bundles, whereas collagen VI is surrounding adipocytes. Despite increased scAT collagen accumulation post-BS, we found decreased collagen I and VI staining at T12 (Supplemental Figure 3), suggesting that increased picrosirius-red

staining may **also** indicate (at least partially) degraded collagen fragments. We tested this hypothesis by measuring collagen fragments with immunostaining, ELISA and zymography from scAT explants. We observed increased stained degraded collagen I surrounding adipocytes in scAT at T3 and T12 (Figure 5E). Accordingly, the concentration of degraded collagen III (C3M) in scAT at T12 was significantly increased compared to T0 (Figure 5F left panel). ProMMP-9 and proMMP-2 entities at 92 kDa and 72 kDa respectively were observed (Figure 5G). Despite individual variability, an increased trend of proMMP-2 at T3 in one non-diabetic obese subject and an increase of proMMP-9 at T3 followed by stabilization at T12 in two others were observed. These changes in proMMPs were not detected in samples from **obese** diabetic subjects **(Figure 5G)**. In parallel, newly synthesized collagen III (Pro-C3M) concentration was significantly decreased in obese compared to non-obese subjects and showed a non-significant increase at T3, T12 (Figure 5F right panel).

DISCUSSION

Collagen accumulation in white AT is considered as an important pathological alteration associated with several comorbidities of obesity (1,7,9). Our results provide new insights into weight-loss induced AT remodeling **in paired humans individuals before and one-year post-BS. Our results** suggest that picrosirius-red stained collagen in scAT does not always refer to "pathological collagens", but could be a signature of extensive tissue remodeling and collagen degradation following adipocyte shrinkage during weight loss along with improved clinical, metabolic and inflammatory outcomes.

During physiological tissue repair, ECM accumulation is a key regenerative step replacing tissue debris and dead cells (2). In pathological conditions, increased collagen deposition is not always synonymous with deleterious fibrosis. In myocardial injury, different types of fibrosis have been reported according to the progression and history of cardiomyopathies: a reactive "interstitial fibrosis" with ECM deposition in response to deleterious stimuli is considered pathological. Conversely, a "replacement fibrosis" that replaces myocytes after cell damage or necrosis may preserve the structural integrity of the myocardium (25,26). As we did not find any association between adipocyte diameter reduction and pericellular collagen increase, we attribute this increased pericellular collagen to "replacement collagen" that occurs at adipocyte shrinkage sites. This is further supported by our observation of some large parenchyma areas filled with less well-organized collagen. This replacement collagen, as part of the remodeling process, might be an adaptive and physiological phenomenon during weight-loss.

Cross-linking is necessary for matrix fibers maturation and stabilization (27) and contributes to increased tissue stiffness. LOX is a major enzyme mediating collagen and elastin cross-linking. A relationship between LOX enzymatic activity and tissue stiffness was established in colorectal cancer and indicated a pivotal role of LOX associated stiffness in driving colorectal cancer progression (12,28). In obese subjects, scAT LOX gene expression is increased (11). Increased perioperative scAT pericellular collagen is associated with increased tissue stiffness measured by Adiposcan™ (9). Moreover, pericellular collagen leads to adipocyte constraints and stimulates genes encoding mechano-sensitive, inflammatory and profibrotic proteins such as CTGF in a 3D model (11). Herein, decreased LOX gene expression and protein, and increased elastin twist structure evaluated by SHG after weight loss clearly suggest decreased cross-linking and relaxed fibers.

ScAT stiffness measured by Adiposcan™ relates to adipose tissue rigidity in severe obesity before weight loss and is associated with picrosirius-red stained collagens and metabolic alterations (9). To our surprise, we found increased post-BS collagen accumulation without significant change in average scAT stiffness measured by Adiposcan™ despite large inter-individual variability. **These results, associated with improved metabolic alterations after BS**, suggest that the major ECM remodeling observed after weight loss might be adaptive. **Two profiles of stiffness changes were observed without significant link with clinical parameters, indicating that further studies are required to investigate the potential implication of different scAT SWS profiles in BS outcomes in larger populations.** Our results also suggest that transient elastography Adiposcan™ might be more sensitive to severe cross-linked and dense fibrosis **(i.e. "pathological fibrosis") as showed in liver stiffness measurements** (29,30), thus explaining why Adiposcan™ fails to detect small decreases in post-BS stiffness or alternatively to quantify adaptive ECM remodeling (**i.e. less cross-linked and more degraded collagens**) not linked to pathological conditions. Therefore, Adiposcan™ might be more appropriate to better stratify obese individuals **before any drastic weight intervention or to non-invasively** predict weight loss outcomes (9), **a feature which needs further study in extended cohorts.** Furthermore, other scAT changes occurring after weight loss might also influence tissue stiffness, such as the amount and types of lipids in adipocyte or scAT vascularization**. In addition,** some genes involved in mechano-transduction pathway YAP/TEAD were unchanged while the downstream profibrotic gene CTGF was down-regulated, suggesting again that weight loss induced increased collagen deposition was not associated with pathological constraint.

The transcriptomic study performed before and one-year post-BS confirmed intense tissue remodeling. These results align with other observations of deceased major ECM gene and profibrotic proteins both after short-term BS-induced weight loss (14) or dietary intervention (31). We, herein, suggest that increased picrosirius-red staining is, at least partially, due to increased degraded collagens (collagen I, III) and eventually less newly synthesized collagens (collagen III) as shown by immunohistochemistry and ELISA. Indeed, we found decreased staining of specific collagens such as collagen I and VI. Importantly, we went beyond the transcriptomic results obtained by McChulloch et al who observed only increased post-BS COL6A3 expression but not other collagen VI alpha chains or their protein content (14). Our microarray analysis displayed different expression changes of collagen VI alpha chain: COL6A1 and COL6A2 decreased whereas COL6A3 increased. It is well known that transcriptomic changes of sub-type chains do not always relate to the same changes at the protein level. According to our immunostaining results, we found less collagen VI surrounding adipocytes post-BS.

Our zymography analysis in scAT revealed the presence of proMMP-2 and/or proMMP-9 proteins in obese non-diabetic subjects. ProMMPs are the inactive zymogen forms. There are growing evidences of the ability of proMMP-2 and proMMP-9 to directly activate classical signaling pathways involved in cell growth, survival, migration, and angiogenesis (32). In metabolically healthy obese individuals, scAT proMMP-9 zymographic activity is increased, suggesting that proMMP-9 might be linked with better metabolic profile (33). **The fact that we did observe a difference in obese diabetic individuals seems to be in accordance with this last point, or could also be due to the effect of anti-diabetic drugs.** Exploring the co-expression of proMMPs and TIMPs in the context of scAT remodeling and improved metabolism deserves further consideration.

The mechanisms leading to fibrosis synthesis and degradation at the cellular level need to be better elineated in AT. AT macrophages (ATM) are triggers of fibrosis (34). We previously showed that both diet and BS-induced weight loss improve inflammatory profiles despite non-negligible inter-individual variations (14,24,35). Here, we observed increased $CD163^+/CD68^+$ ratio due to increased $CD163^+$ cells and decreased $CD68^+$cells during weight loss, a profile of activated state of ATM shifted towards M2 relative to M1, as previously shown after 3 months post-BS (24). In addition, $CD163^+$ cells before BS associated with pericellular collagen accumulation, indicating a role in the generation of fibrosis in obese scAT. M2 cells have a complex role in tissue repair and fibrosis: besides direct effects of M2 cells on promoting and suppressing collagen synthesis and fibrosis development, M2 cells are inducers of Treg cells, which are implicated in fibrosis suppression and can directly

produce MMPs and TIMPs, thus controlling ECM turnover (36). The reason why we found a significant negative association between $CD163^+$ cells and collagen accumulation at T12 is unknown, but may suggest a balanced involvement of several cell types during this remodeling process and warrants further exploration. **A number of studies have previously described changes of scAT immune cells quantified by IHC before and after weight loss (14,24,35). However, due to the clinical difficulties in acquiring sufficient and repeated post-surgery scAT surgical biopsy samples in obese subjects during the follow-up, it was hard to compare our IHC observation to other methods such as fluorescence-activated cell sorting (FACS) for quantifying immune cells infiltration.**

Some questions remain unanswered. **Our clinical study aimed at evaluating the changes in scAT ECM until one year, the nadir point of post- BS weight loss in most individuals** (37)**.** The kinetic changes (amount, type, cross-linking) of collagen fibers with longer duration of post-BS weight loss, stabilization, or weight regain remains to evaluate. **Some studies showed interesting results. For example, after** two years post-BS weight stabilization, ex-obese subjects still presented the same amount of picrosirius-red stained scAT fibrosis as morbidly obese subjects, **despite improvements in adipocyte hypertrophy and inflammation infiltration** (38). **However, this ex-obese group was compared to an independent group of pre-BS obese individuals. Specific comparision between two independent groups of patients before and after surgery might induce bias in the results due to important inter-variability in AT fibrosis. Therefore, these findings should be confirmed in samples from same individuals obtained before and after BS, as we herein assessed. Furthermore,** the type of collagens and cross-linking enzymes were not investigated. **In addition,** obese subjects experience periods of weight fluctuations even post-BS (37) that could possibly subsequently modify their adipose tissue ECM characteristics. We previously showed that 59 subjects who underwent RYGB after an initial failure of gastric banding displayed significantly higher total collagen accumulation than primarily operated subjects (9), suggesting again that weight fluctuations impact on ECM remodeling. **Therefore, it is of interest to pursue the follow-up of our obese subjects, who were already investigated at baseline and up until one year, to evaluate longer-term scAT remodeling and potential relationships with BS outcomes. In addition, there is hardly any current data concerning the change of visceral adipose tissue characteristics. In one human study, obese subjects displayed decreased fat diameter in visceral AT as measured by ultrasound (39). In rodent models, mice who underwent BS demonstrated decreased infiltration of T-lymphocytes and macrophages in visceral AT (40).**

Further study in these post-BS features in humans would be of major interest. However, there are clinical and ethical limitations to such explorations and the development of non-invasive (e.g. imaging) measures are indispensable.

In conclusion, this study provides new insights into scAT adaptation during drastic weight-loss and shows that increased picrosirius-red staining is a signature of tissue remodeling with increased collagen degradation and less cross-linked fibers. It will be critical to follow patients during long-term weight loss and to determine the impact of scAT remodeling on metabolic improvements.

Acknowledgements. We are grateful to the patients who contributed to this work and especially those who accepted repeated surgical biopsies during the follow-up. We thank Valentine Lemoine for patients' follow-up, Florence Marchelli for data management, and Rohia Alili for her contribution in bio-banking. We thank Frédéric Charlotte, Annette Lescot and Anne Gloaguen for scAT tissue preparation and picrosirius-red staining. We thank Victoria Dubar for helping in immunohistostaining. We thank Claire Lovo, Aurélien Dauphin, and Christophe Klein for performing SHG acquisition and for their help in analysis (Imaging Facilities, Institut du Cerveau et de la Moelle épinière, PitiéSalpétrière, Paris, France). We thank Brandon Kayser, Institute of Cardiometabolism and Nutrition (ICAN), for editorial/writing support.

References

1. **Sun K, Tordjman J, Clément K, Scherer PE.** Fibrosis and Adipose Tissue Dysfunction. *Cell Metab.* 2013;18(4):470–477.

2. **Duffield JS, Lupher M, Thannickal VJ, Wynn TA.** Host Responses in Tissue Repair and Fibrosis. *Annu. Rev. Pathol. Mech. Dis.* 2013;8(1):241–276.

3. **Chun T-H, Hotary KB, Sabeh F, Saltiel AR, Allen ED, Weiss SJ.** A Pericellular Collagenase Directs the 3-Dimensional Development of White Adipose Tissue. *Cell* 2006;125(3):577–591.

4. **Pasarica M, Gowronska-Kozak B, Burk D, Remedios I, Hymel D, Gimble J, Ravussin E, Bray GA, Smith SR.** Adipose Tissue Collagen VI in Obesity. *J. Clin. Endocrinol. Metab.* 2009;94(12):5155–5162.

5. **Spencer M, Yao-Borengasser A, Unal R, Rasouli N, Gurley CM, Zhu B, Peterson CA, Kern PA.** Adipose tissue macrophages in insulin-resistant subjects are associated with collagen VI and fibrosis and demonstrate alternative activation. *AJP Endocrinol. Metab.* 2010;299(6):E1016–E1027.

6. **Khan T, Muise ES, Iyengar P, Wang ZV, Chandalia M, Abate N, Zhang BB, Bonaldo P, Chua S, Scherer PE.** Metabolic Dysregulation and Adipose Tissue Fibrosis: Role of Collagen VI. *Mol. Cell. Biol.* 2009;29(6):1575–1591.

7. **Divoux A, Tordjman J, Lacasa D, Veyrie N, Hugol D, Aissat A, Basdevant A, Guerre-Millo M, Poitou C, Zucker J-D, others.** Fibrosis in human adipose tissue: composition, distribution, and link with lipid metabolism and fat mass loss. *Diabetes* 2010;59(11):2817–2825.

8. **Henegar C, Tordjman J, Achard V, Lacasa D, Cremer I, Guerre-Millo M, Poitou C, Basdevant A, Stich V, Viguerie N, others.** Adipose tissue transcriptomic signature highlights the pathological relevance of extracellular matrix in human obesity. *Genome Biol.* 2008;9(1):R14.

9. **Abdennour M, Reggio S, Le Naour G, Liu Y, Poitou C, Aron-Wisnewsky J, Charlotte F, Bouillot J-L, Torcivia A, Sasso M, Miette V, Zucker J-D, Bedossa P, Tordjman J, Clement K.** Association of Adipose Tissue and Liver Fibrosis With Tissue Stiffness in Morbid Obesity: Links With Diabetes and BMI Loss After Gastric Bypass. *J. Clin. Endocrinol. Metab.* 2014;99(3):898–907.

10. **Venteclef N, Guglielmi V, Balse E, Gaborit B, Cotillard A, Atassi F, Amour J, Leprince P, Dutour A, Clement K, Hatem SN.** Human epicardial adipose tissue induces fibrosis of the atrial myocardium through the secretion of adipo-fibrokines. *Eur. Heart J.* 2015;36(13):795–805.

11. **Pellegrinelli V, Heuvingh J, du Roure O, Rouault C, Devulder A, Klein C, Lacasa M, Clément E, Lacasa D, Clément K.** Human adipocyte function is impacted by mechanical cues. *J. Pathol.* 2014;233(2):183–195.

12. **Baker AM, Bird D, Lang G, Cox TR, Erler JT.** Lysyl oxidase enzymatic function increases stiffness to drive colorectal cancer progression through FAK. *Oncogene* 2013;32(14):1863–1868.

13. **Halberg N, Khan T, Trujillo ME, Wernstedt-Asterholm I, Attie AD, Sherwani S, Wang ZV, Landskroner-Eiger S, Dineen S, Magalang UJ, Brekken RA, Scherer PE.** Hypoxia-Inducible Factor 1 Induces Fibrosis and Insulin Resistance in White Adipose Tissue. *Mol. Cell. Biol.* 2009;29(16):4467–4483.

14. **Cancello R, Henegar C, Viguerie N, Taleb S, Poitou C, Rouault C, Coupaye M, Pelloux V, Hugol D, Bouillot J-L, Bouloumié A, Barbatelli G, Cinti S, Svensson P-A, Barsh GS, Zucker J-D, Basdevant A, Langin**

D, Clément K. Reduction of macrophage infiltration and chemoattractant gene expression changes in white adipose tissue of morbidly obese subjects after surgery-induced weight loss. *Diabetes* 2005;54(8):2277–2286.

15. **Genser L, Vatier C, Keophyphath M, Aron-Wisnewsky J, Poitou C, Clément K, Bastard J-P.** Le prélèvement de tissu adipeux: un acte médical pour la recherche clinique. Perspectives pour le soin courant. *Obésité* 2013;8(4):222–227.

16. **Mutch DM, Tordjman J, Pelloux V, Hanczar B, Henegar C, Poitou C, Veyrie N, Zucker J-D, Clement K.** Needle and surgical biopsy techniques differentially affect adipose tissue gene expression profiles. *Am. J. Clin. Nutr.* 2008;89(1):51–57.

17. **Matthews DR, Hosker JP, Rudenski AS, Naylor BA, Treacher DF, Turner RC.** Homeostasis model assessment: insulin resistance and beta-cell function from fasting plasma glucose and insulin concentrations in man. *Diabetologia* 1985;28(7):412–419.

18. **Sandrin L, Fourquet B, Hasquenoph J-M, Yon S, Fournier C, Mal F, Christidis C, Ziol M, Poulet B, Kazemi F, Beaugrand M, Palau R.** Transient elastography: a new noninvasive method for assessment of hepatic fibrosis. *Ultrasound Med. Biol.* 2003;29(12):1705–1713.

19. **Sasso M, Abdennour M, Liu Y, Clet M, Bouillot J-L, Le Naour G, Bedossa P, Wisnewsky JA, Tordjman J, Clement K, Miette V.** AdipoScan (TM) - A novel transient elastography based tool to assess subcutaneous adipose tissue shear wave speed in morbidly obese patients. *2014 Ieee Int. Ultrason. Symp. Ius* 2014:1124–1127.

20. **Lacroix D, Moutel S, Coupaye M, Huvenne H, Faucher P, Pelloux V, Rouault C, Bastard J-P, Cagnard N, Dubern B, Clément K, Poitou C.** Metabolic and adipose tissue signatures in adults with Prader-Willi syndrome: a model of extreme adiposity. *J. Clin. Endocrinol. Metab.* 2015;100(3):850–859.

21. **Cancello R, Tordjman J, Poitou C, Guilhem G, Bouillot JL, Hugol D, Coussieu C, Basdevant A, Hen AB, Bedossa P, Guerre-Millo M, Clément K.** Increased Infiltration of Macrophages in Omental Adipose Tissue Is Associated With Marked Hepatic Lesions in Morbid Human Obesity. *Diabetes* 2006;55(6):1554–1561.

22. **Bay-Jensen AC, Leeming DJ, Kleyer A, Veidal SS, Schett G, Karsdal MA.** Ankylosing spondylitis is characterized by an increased turnover of several different metalloproteinase-derived collagen species: a cross-sectional study. *Rheumatol. Int.* 2012;32(11):3565–3572.

23. **Bauvois B, Dumont J, Mathiot C, Kolb JP.** Production of matrix metalloproteinase-9 in early stage B-CLL: suppression by interferons. *Leukemia* 2002;16(5):791–798.

24. **Aron-Wisnewsky J, Tordjman J, Poitou C, Darakhshan F, Hugol D, Basdevant A, Aissat A, Guerre-Millo M, Clément K.** Human Adipose Tissue Macrophages: M1 and M2 Cell Surface Markers in Subcutaneous and Omental Depots and after Weight Loss. *J. Clin. Endocrinol. Metab.* 2009;94(11):4619–4623.

25. **Longo DL, Rockey DC, Bell PD, Hill JA.** Fibrosis — A Common Pathway to Organ Injury and Failure. *N. Engl. J. Med.* 2015;372(12):1138–1149.

26. **Mewton N, Liu CY, Croisille P, Bluemke D, Lima JAC.** Assessment of Myocardial Fibrosis With Cardiovascular Magnetic Resonance. *J. Am. Coll. Cardiol.* 2011;57(8):891–903.

27. **Myllyharju J.** Intracellular Post-Translational Modifications of Collagens. In: Brinckmann J, Notbohm H, Müller PK, eds. *Collagen*. Topics in Current Chemistry. Springer Berlin Heidelberg; 2005:115–147.

28. **Levental KR, Yu H, Kass L, Lakins JN, Egeblad M, Erler JT, Fong SFT, Csiszar K, Giaccia A, Weninger W, Yamauchi M, Gasser DL, Weaver VM.** Matrix Crosslinking Forces Tumor Progression by Enhancing Integrin Signaling. *Cell* 2009;139(5):891–906.

29. **Afdhal NH, Bacon BR, Patel K, Lawitz EJ, Gordon SC, Nelson DR, Challies TL, Nasser I, Garg J, Wei L-J, McHutchison JG.** Accuracy of Fibroscan, Compared With Histology, in Analysis of Liver Fibrosis in Patients With Hepatitis B or C: A United States Multicenter Study. *Clin. Gastroenterol. Hepatol.* 2015;13(4):772–779.e3.

30. **Grenard P, Bresson-Hadni S, El Alaoui S, Chevallier M, Vuitton DA, Ricard-Blum S.** Transglutaminase-mediated cross-linking is involved in the stabilization of extracellular matrix in human liver fibrosis. *J. Hepatol.* 2001;35(3):367–375.

31. **Kolehmainen M, Salopuro T, Schwab US, Kekäläinen J, Kallio P, Laaksonen DE, Pulkkinen L, Lindi VI, Sivenius K, Mager U, others.** Weight reduction modulates expression of genes involved in extracellular matrix and cell death: the GENOBIN study. *Int. J. Obes.* 2008;32(2):292–303.

32. **Bauvois B.** New facets of matrix metalloproteinases MMP-2 and MMP-9 as cell surface transducers: Outside-in signaling and relationship to tumor progression. *Biochim. Biophys. Acta BBA - Rev. Cancer* 2012;1825(1):29–36.

33. **Lackey DE, Burk DH, Ali MR, Mostaedi R, Smith WH, Park J, Scherer PE, Seay SA, McCoin CS, Bonaldo P, Adams SH.** Contributions of adipose tissue architectural and tensile properties toward defining healthy and unhealthy obesity. *AJP Endocrinol. Metab.* 2014;306(3):E233–E246.

34. **Keophiphath M, Achard V, Henegar C, Rouault C, Clément K, Lacasa D.** Macrophage-Secreted Factors Promote a Profibrotic Phenotype in Human Preadipocytes. *Mol. Endocrinol.* 2009;23(1):11–24.

35. **Clement K.** Weight loss regulates inflammation-related genes in white adipose tissue of obese subjects. *FASEB J.* 2004;18(14):1657–1669.

36. **Murray PJ, Wynn TA.** Protective and pathogenic functions of macrophage subsets. *Nat. Rev. Immunol.* 2011;11(11):723–737.

37. **Sjöström L.** Review of the key results from the Swedish Obese Subjects (SOS) trial - a prospective controlled intervention study of bariatric surgery. *J. Intern. Med.* 2013;273(3):219–234.

38. **Cancello R, Zulian A, Gentilini D, Mencarelli M, Della Barba A, Maffei M, Vitti P, Invitti C, Liuzzi A, Di Blasio AM.** Permanence of molecular features of obesity in subcutaneous adipose tissue of ex-obese subjects. *Int. J. Obes.* 2013;37(6):867–873.

39. **Tschoner A, Sturm W, Engl J, Kaser S, Laimer M, Laimer E, Klaus A, Patsch JR, Ebenbichler CF.** Plasminogen activator inhibitor 1 and visceral obesity during pronounced weight loss after bariatric surgery. *Nutr. Metab. Cardiovasc. Dis.* 2012;22(4):340–346.

40. **Zhang H, Wang Y, Zhang J, Potter BJ, Sowers JR, Zhang C.** Bariatric Surgery Reduces Visceral Adipose Inflammation and Improves Endothelial Function in Type 2 Diabetic Mice. *Arterioscler. Thromb. Vasc. Biol.* 2011;31(9):2063–2069.

Legende

Table 1

Values are expressed as means ± SD (standard deviation), unless otherwise stated. hsCRP, highly sensitive C-reactive protein; HOMA-IR, homeostatic model assessment-insulin resistance; HOMA-B (%), beta cell function; HOMA-S (%): insulin sensitivity. There are 11 common subjects in Group1 and Group2. For continuous data, repeated ANOVA was used to compare three time points in Group1 and Group2, when p values of ANOVA were <0.05, Holm-Sidak's parametric multiple comparison test was used to compare each of the two time points; student's t-test was used in Group3. For categorical data, Fisher's exact test was used. * $p<0.05$ when compared to T0 in each group, # $p<0.05$ when compared to T3 in Group1 and Group2. Subjects' baseline characteristics (T0) in three groups were compared by ANOVA for quantitative data and by Fisher's exact test for qualitative data. No significant differences were found except the BS type.

Figure Legends

Figure 1. Study flowchart of 118 obese subjects.

Three groups of obese individuals were recruited for scAT exploration at baseline (T0) and during the follow-up after bariatric surgery at 3 monthsT3 and 12 months (T12). There are 11 common subjects (female n=6) in Group1 and Group2 in whom we performed both histological analysis (P-R, IHC) and scAT stiffness measurement (Stiffness). **A sub-group of 14 subjects in Group 2 underwent scAT needle aspiration for RT-PCR analysis.** ScAT, subcutaneous adipose tissue; P-R, Picrosirius-red staining; IHC, immunohistochemistry; SHG, second harmonic generation.

Figure 2. ScAT evaluation.

Collagen accumulation in scAT stained by picrosirius-red in one representative obese subject at baseline (T0) (A), 3 months (T3) (B) and 12 months (T12) (C) post-BS. Total and pericellular collagen accumulation (D) and adipocyte size (E) at T0, T3 and T12 in 36 obese subjects from Group1. Repeated ANOVA test and Holm-Sidak's parametric multiple comparison test were used, * $p<0.01$. F, scAT stiffness, shear wave speed (SWS), was evaluated at T0, T3 and T12 post-BS measured by transient elastography in 35 subjects (Group2). Repeated ANOVA test, $p > 0.05$. **G, scAT stiffness trajectories are clustered by K-means for longitudinal data (KmL), two major clusters (A and B) of stiffness change are observed. No significant difference of stiffness at T3 was observed between these two clusters (Cluster A 0.89±0.33 vs. cluster B 0.86±0.15, Wilcoxon test p=0.63)**

Figure 3 Macrophage infiltration in scAT

Evolution of $CD163^+/CD68^+$ ratio (A) and $CD163^+$ cells (B) and $CD68^+$ cells (C) in scAT evaluated by immunohistochemistry **(IHC)** at baseline (T0) and 12 months post-BS (T12) in 15 obese subjects from Group1 (IHC T0-T3-T12 sub-group). Solid lines represent non-diabetic subjects (n=8), dotted lines represent type-2 diabetic subjects (n=7). Pearson's correlation between $CD163^+$ cells and pericellular collagen accumulation at baseline (T0) (D left panel) and 12months after BS (T12) (D right panel), hollow points represent Type-2 diabetic subjects.

Figure 4. Transcriptomic signature of scAT ECM genes in obese subjects one year after BS

Gene expression levels from micro-array data in scAT at baseline represented as dotted line (T0) and 12 months post-BS (T12) represented as bars, in 42 women from Group3: A, genes involved in ECM remodeling (matrix fibers, cross linking, profibrotic protein, degradation proteins and adhesion protein) show important changes. B, most genes involved in post-transcriptional modifications of collagen are down regulated one year post-BS. They include i) enzymes involved in the hydroxylation of proline: prolyl 4-hydroxylase; prolyl-3 hydrolase;ii) enzyme involved in glycosylation of hydroxylysine: GLT25D1;iii) chaperon molecules HSP47, GRP94, calexin (CANX) and disulphideisomerase (PDI) (HSPA5, DNAJC10, ERP29, PDIA4, PDIA6) and iv) enzymes involved in N- and C- propeptides of procollagens: ADAMTS1, ADAMTS2, ADAMTS5, ADAMTSL4. By contrast, prolyl-3 hydrolase (P3H2, P3H3) and ADAMTS9 genes were up-regulated. Data are presented as changes from baseline. *$p<0.05$.

Figure 5. Cross-linking of Matrix Fibers and collagen degradation and synthesis in scAT.

A, Lysyl oxidase (LOX) gene expression levels at baseline (T0), 3 months (T3) and 12 months (T12) post-BS in 14 obese non-diabetic women from Group2. B, LOX stained by immunohistochemistry in obese and non-obese subjects, X20. C, scAT elastin structure (magenta) was observed by second harmonic generation at T0 and T3 in one representative obese subject among the three, X20. D, correlation heatmap between changes of bioclinical parameters and changes of genes regulating cross-linking from T0 to T12 in 42 women from Group3. Correlations between gene expression and changes of HbA1c and glycemia were analyzed separately in non-diabetic (nonDM, n=28) and Type-2 diabetic (DM, n=14) subjects. HOMA-IR, HOMA-B% and HOMA-S% were only analyzed in non-diabetic subjects. Pearson's coefficients of each correlation are represented as blue (negative correlation) or red (positive correlation), * $p<0.05$. E, degraded collagen I in scAT stained by immunohistochemistry in one representative obese subject at T0, T3 and T12 and one representative non-obese subject. F, degraded collagen III (left panel) and newly synthesized collagen III (right panel) in scAT explant measured by ELISA in 5 non obese (Non Ob) and 10 obese subjects (Group1). Diabetic subjects are in red, * $p<0.05$. G, analysis of (pro)MMP-2 and (pro)MMP-9 presence in scAT by gelatin zymography **in 3 obese non-diabetic (Ob), 3 obese diabetic (Ob Diab) and 2 non-obese subjects. Ob Diab 1 was under metformin at T0, but not treated at T3, T12; Ob Diab 2 was under sitagliptin, glimepiride, metaformin at T0, metformin at T3, not treated at T12; Ob Diab 3 were under**

insulin, liraglutide, glimepiride and metformin at T0, insulin, metformin at T3, glimepiride and metformin at T12. U937 cells (ATCC CRL-1593.2) stimulated with 100 U/ml recombinant TNF for 48 h were used as positive control. ProMMP-2 (72kDa) and proMMP-9 (92 kDa) were detected as transparent bands on the background of Eza-blue stained gelatin.

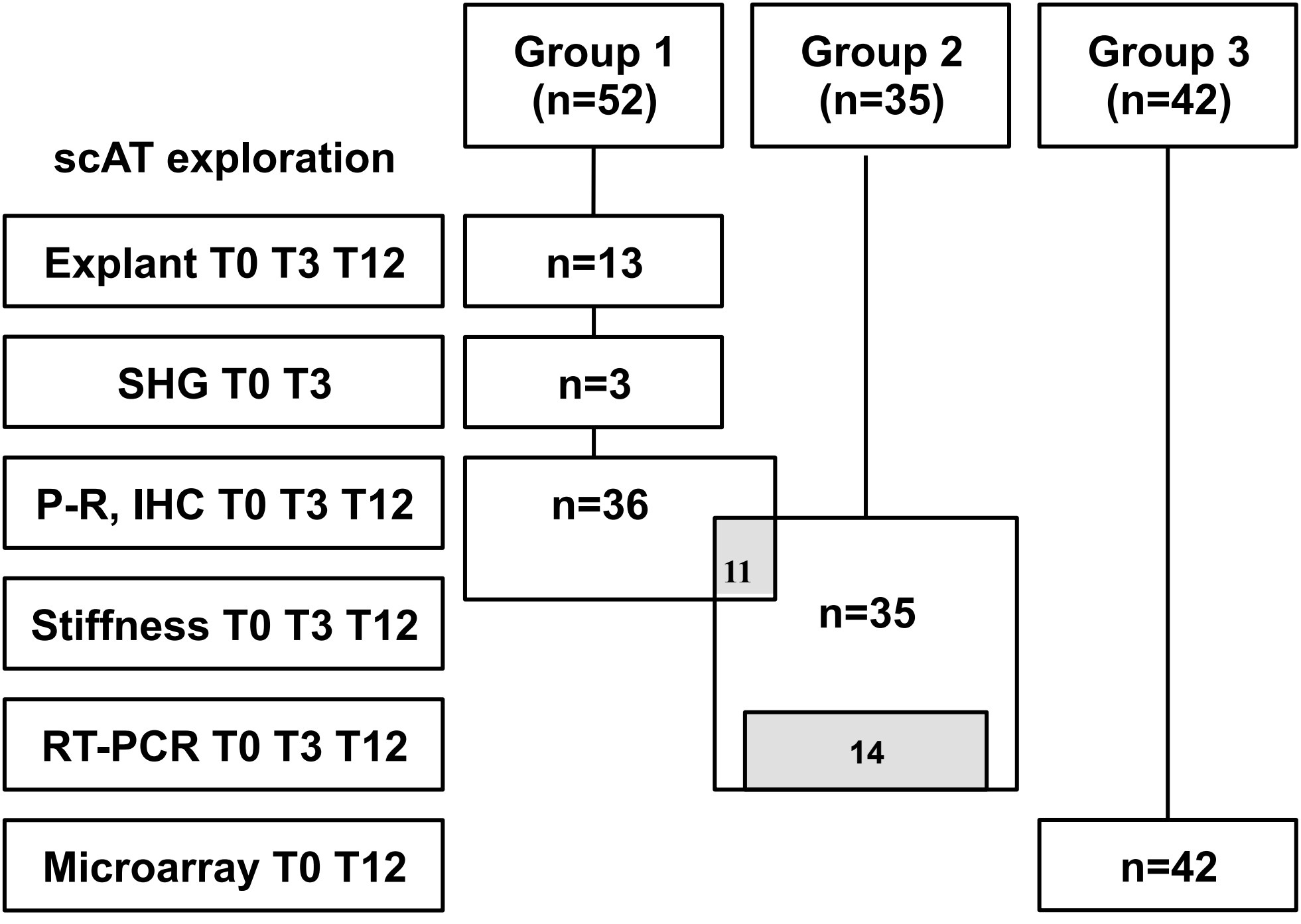
Group 1
(n=52)
Group 2
(n=35)
Group 3
(n=42)
scAT exploration
Explant T0 T3 T12
n=13
SHG T0 T3
n=3
P-R, IHC T0 T3 T12
n=36
11
n=35
Stiffness T0 T3 T12
RT-PCR T0 T3 T12
14
Microarray T0 T12
n=42

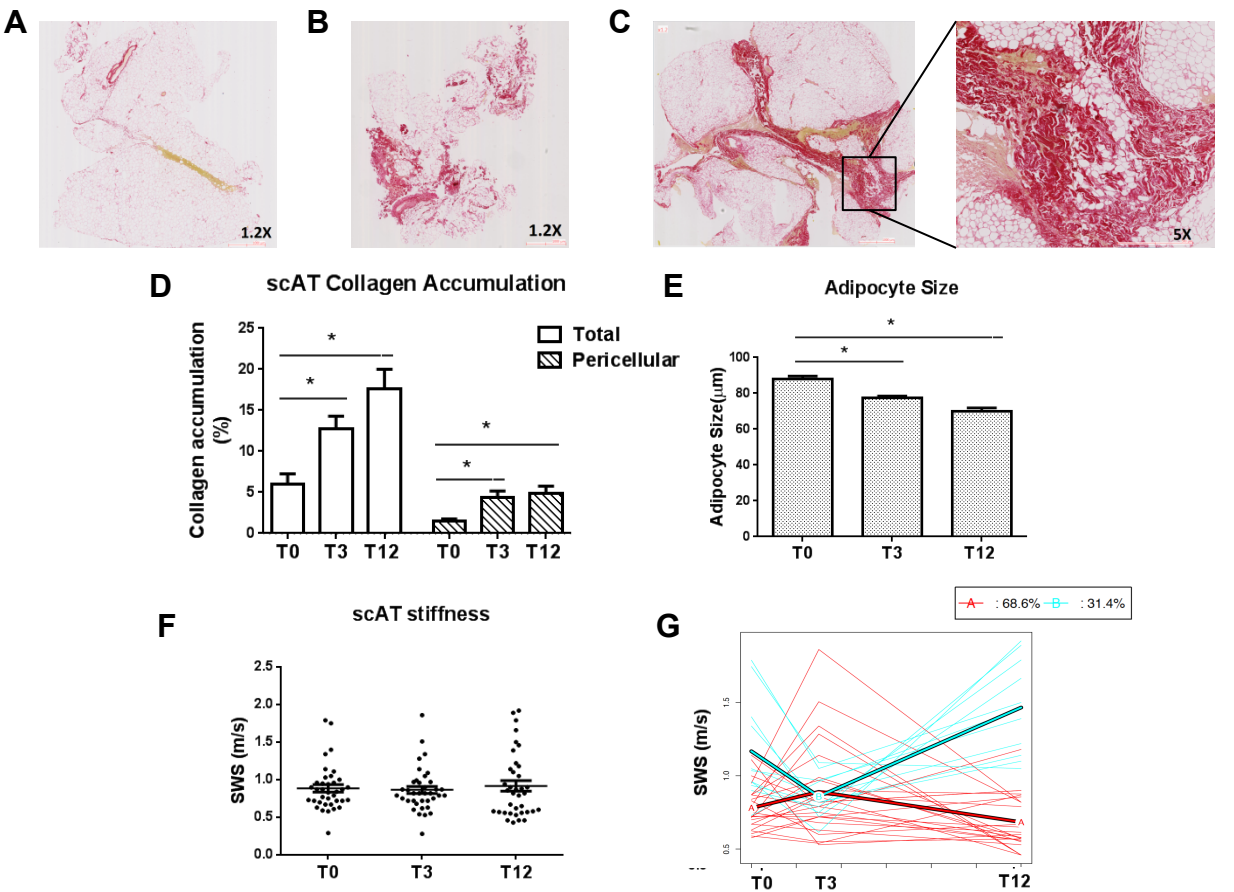
A
1.2X
B
1.2X
C
5X
D
scAT Collagen Accumulation
Collagen accumulation (%)
Total
Pericellular
T0
T3
T12
E
Adipocyte Size
Adipocyte Size(μm)
F
scAT stiffness
SWS (m/s)
G
A : 68.6%
B : 31.4%
SWS (m/s)

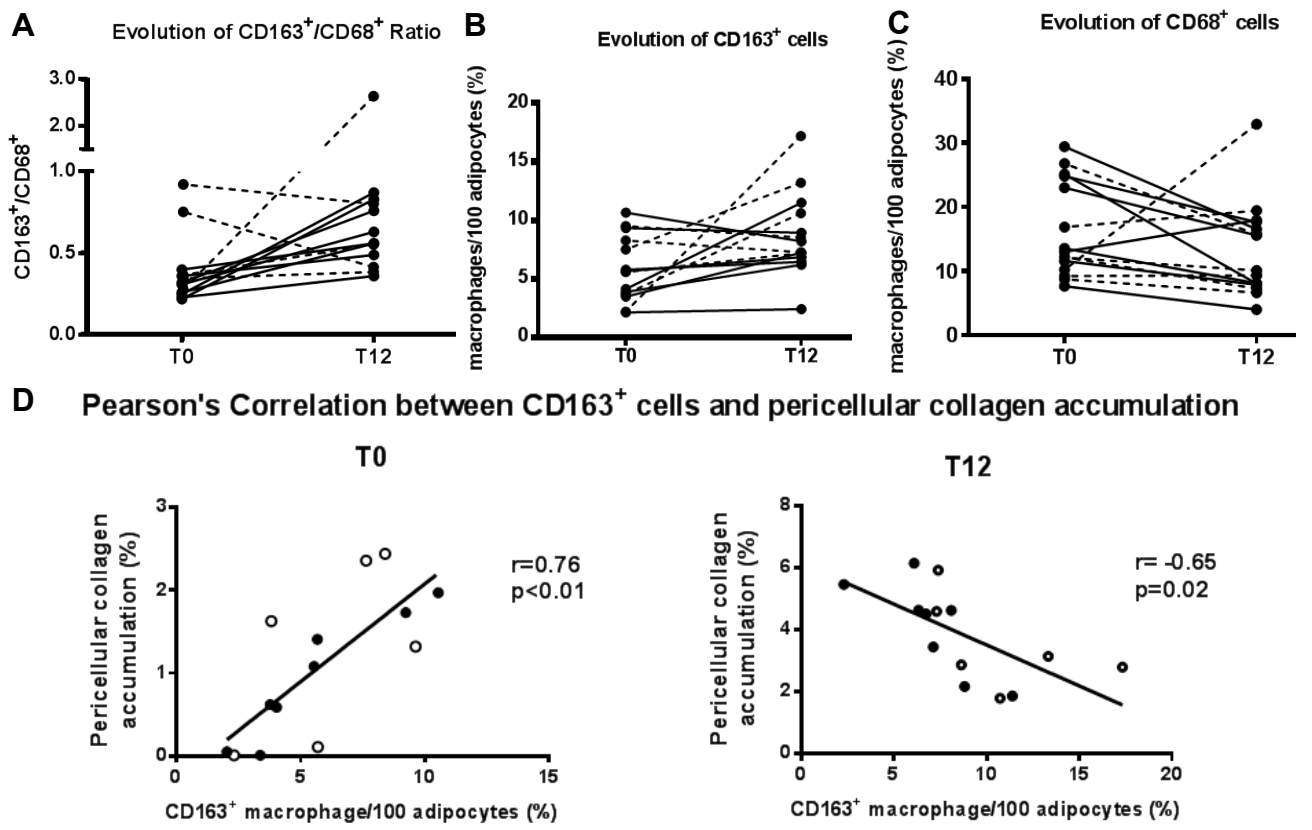
A
Evolution of CD163+/CD68+ Ratio
CD163+/CD68+
3.0
2.0
1.0
0.5
0.0
T0
T12
B
Evolution of CD163+ cells
macrophages/100 adipocytes (%)
20
15
10
5
0
T0
T12
C
Evolution of CD68+ cells
macrophages/100 adipocytes (%)
40
30
20
10
0
T0
T12
D
Pearson's Correlation between CD163+ cells and pericellular collagen accumulation
T0
Pericellular collagen accumulation (%)
r=0.76
p<0.01
CD163+ macrophage/100 adipocytes (%)
T12
Pericellular collagen accumulation (%)
r= -0.65
p=0.02
CD163+ macrophage/100 adipocytes (%)

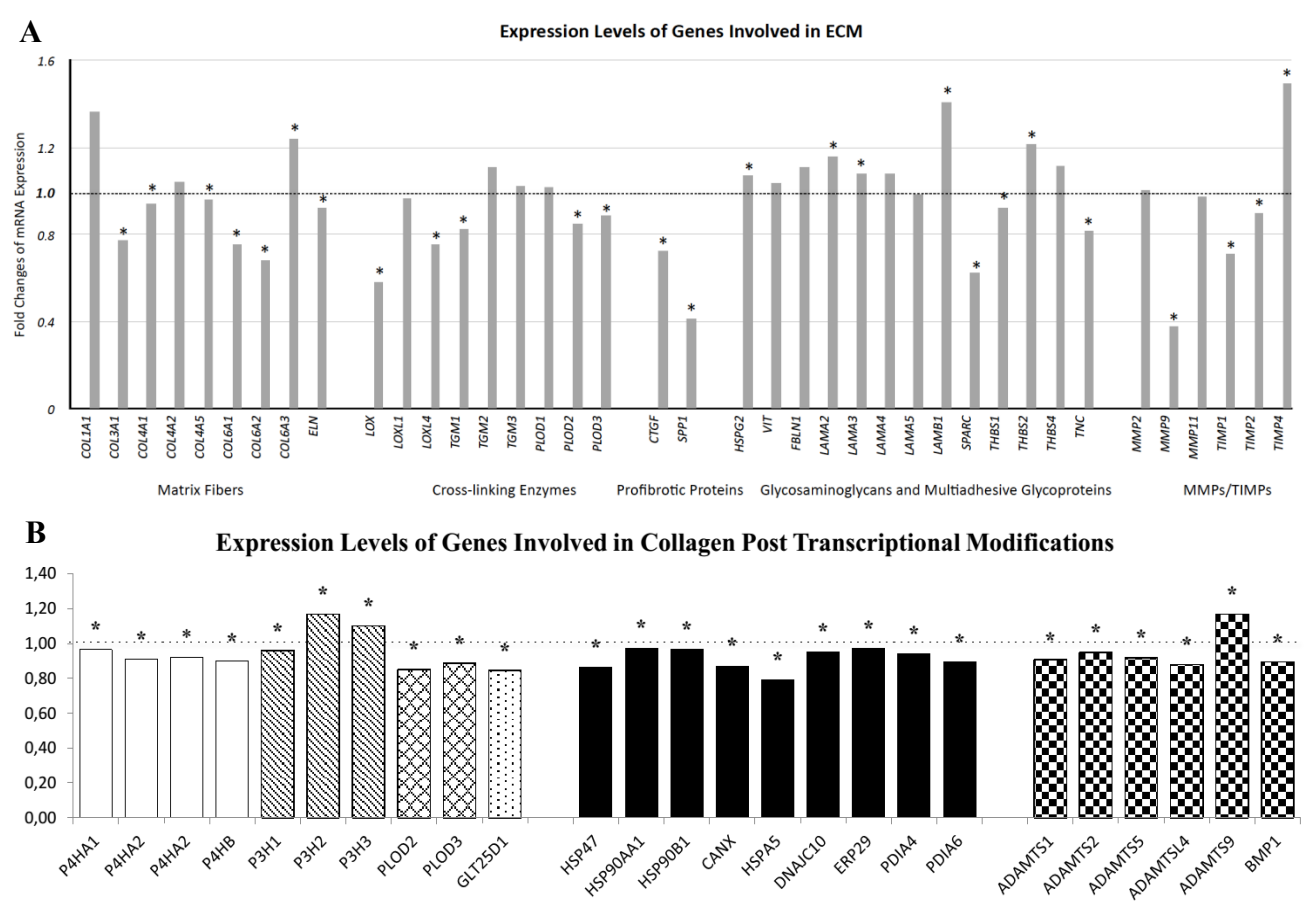
A
Expression Levels of Genes Involved in ECM
Fold Changes of mRNA Expression
1.6
1.2
1.0
0.8
0.4
0
COL1A1
COL3A1
COL4A1
COL4A2
COL4A5
COL6A1
COL6A2
COL6A3
ELN
LOX
LOXL1
LOXL4
TGM1
TGM2
TGM3
PLOD1
PLOD2
PLOD3
CTGF
SPP1
HSPG2
VIT
FBLN1
LAMA2
LAMA3
LAMA4
LAMA5
LAMB1
SPARC
THBS1
THBS2
THBS4
TNC
MMP2
MMP9
MMP11
TIMP1
TIMP2
TIMP4
Matrix Fibers
Cross-linking Enzymes
Profibrotic Proteins
Glycosaminoglycans and Multiadhesive Glycoproteins
MMPs/TIMPs
B
Expression Levels of Genes Involved in Collagen Post Transcriptional Modifications
1,40
1,20
1,00
0,80
0,60
0,40
0,20
0,00
P4HA1
P4HA2
P4HA2
P4HB
P3H1
P3H2
P3H3
PLOD2
PLOD3
GLT25D1
HSP47
HSP90AA1
HSP90B1
CANX
HSPA5
DNAJC10
ERP29
PDIA4
PDIA6
ADAMTS1
ADAMTS2
ADAMTS5
ADAMTSL4
ADAMTS9
BMP1

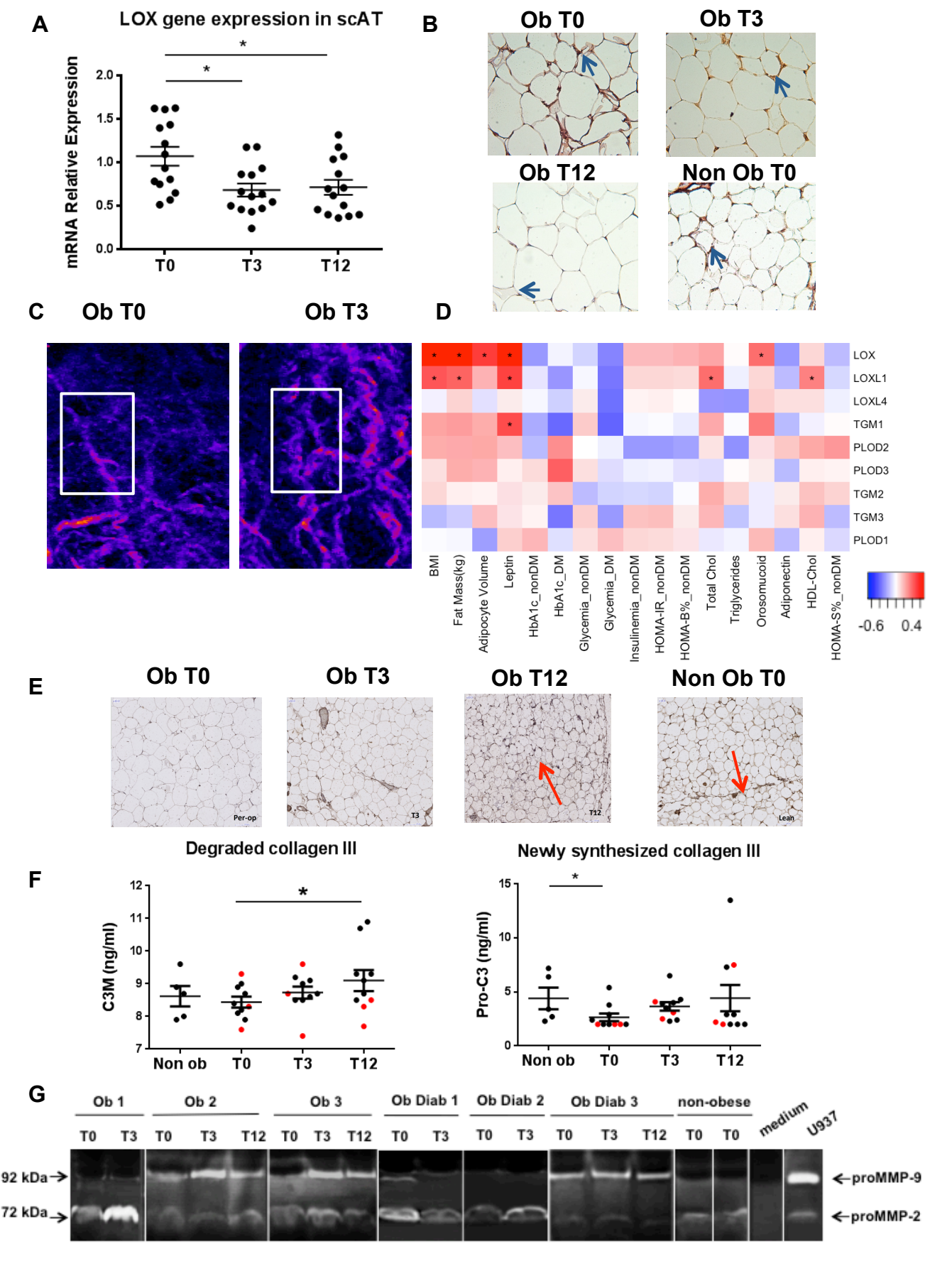
A
LOX gene expression in scAT
mRNA Relative Expression
2.0
1.5
1.0
0.5
0.0
T0
T3
T12
B
Ob T0
Ob T3
Ob T12
Non Ob T0
C
Ob T0
Ob T3
D
LOX
LOXL1
LOXL4
TGM1
PLOD2
PLOD3
TGM2
TGM3
PLOD1
BMI
Fat Mass(kg)
Adipocyte Volume
Leptin
HbA1c_nonDM
HbA1c_DM
Glycemia_nonDM
Glycemia_DM
Insulinemia_nonDM
HOMA-IR_nonDM
HOMA-B%_nonDM
Total Chol
Triglycerides
Orosomucoid
Adiponectin
HDL-Chol
HOMA-S%_nonDM
-0.6
0.4
E
Ob T0
Ob T3
Ob T12
Non Ob T0
Per-op
T3
T12
Lean
Degraded collagen III
Newly synthesized collagen III
F
C3M (ng/ml)
12
11
10
9
8
7
Non ob
T0
T3
T12
Pro-C3 (ng/ml)
15
10
5
0
Non ob
T0
T3
T12
G
Ob 1
Ob 2
Ob 3
Ob Diab 1
Ob Diab 2
Ob Diab 3
non-obese
T0
T3
T0
T3
T12
T0
T3
T12
T0
T3
T0
T3
T0
T3
T12
T0
T0
medium
U937
92 kDa
72 kDa
proMMP-9
proMMP-2

A

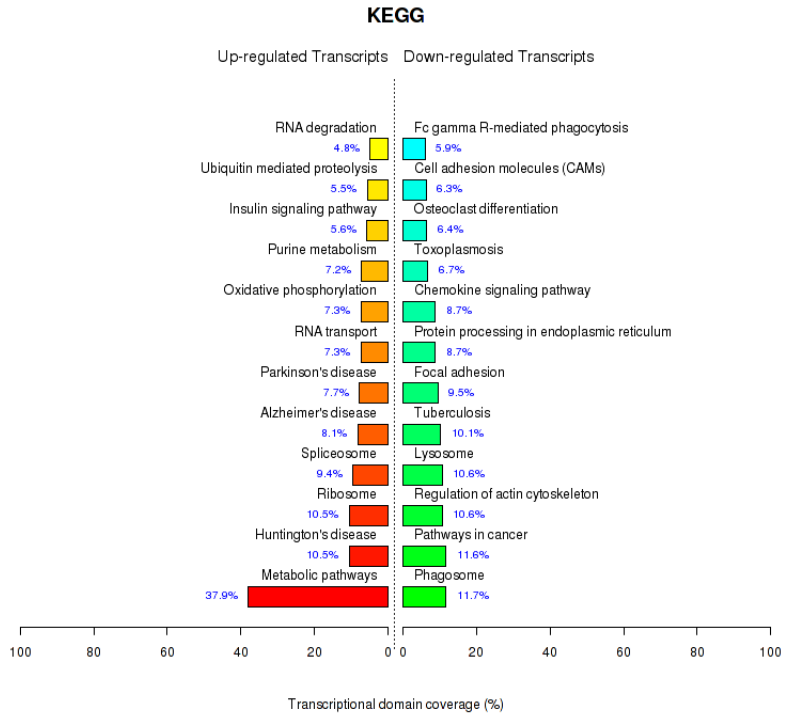
KEGG
Up-regulated Transcripts
Down-regulated Transcripts
RNA degradation
4.8%
Ubiquitin mediated proteolysis
5.5%
Insulin signaling pathway
5.6%
Purine metabolism
7.2%
Oxidative phosphorylation
7.3%
RNA transport
7.3%
Parkinson's disease
7.7%
Alzheimer's disease
8.1%
Spliceosome
9.4%
Ribosome
10.5%
Huntington's disease
10.5%
Metabolic pathways
37.9%
Fc gamma R-mediated phagocytosis
5.9%
Cell adhesion molecules (CAMs)
6.3%
Osteoclast differentiation
6.4%
Toxoplasmosis
6.7%
Chemokine signaling pathway
8.7%
Protein processing in endoplasmic reticulum
8.7%
Focal adhesion
9.5%
Tuberculosis
10.1%
Lysosome
10.6%
Regulation of actin cytoskeleton
10.6%
Pathways in cancer
11.6%
Phagosome
11.7%
100
80
60
40
20
0
0
20
40
60
80
100
Transcriptional domain coverage (%)

B

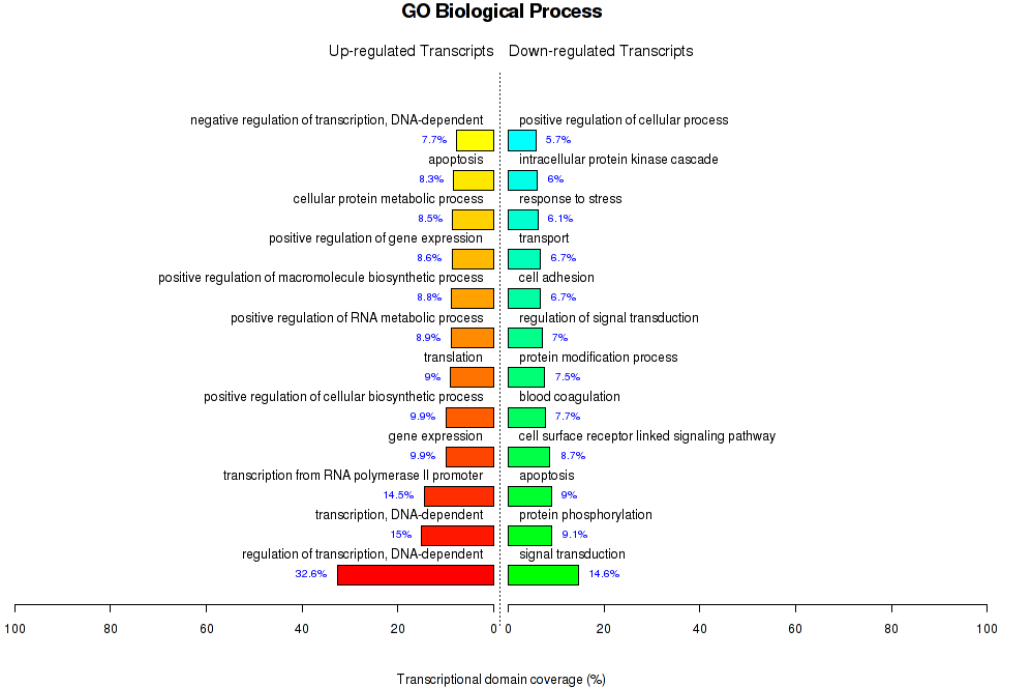
GO Biological Process
Up-regulated Transcripts
Down-regulated Transcripts
negative regulation of transcription, DNA-dependent
7.7%
apoptosis
8.3%
cellular protein metabolic process
8.5%
positive regulation of gene expression
8.6%
positive regulation of macromolecule biosynthetic process
8.8%
positive regulation of RNA metabolic process
8.9%
translation
9%
positive regulation of cellular biosynthetic process
9.9%
gene expression
9.9%
transcription from RNA polymerase II promoter
14.5%
transcription, DNA-dependent
15%
regulation of transcription, DNA-dependent
32.6%
positive regulation of cellular process
5.7%
intracellular protein kinase cascade
6%
response to stress
6.1%
transport
6.7%
cell adhesion
6.7%
regulation of signal transduction
7%
protein modification process
7.5%
blood coagulation
7.7%
cell surface receptor linked signaling pathway
8.7%
apoptosis
9%
protein phosphorylation
9.1%
signal transduction
14.6%
100
80
60
40
20
0
0
20
40
60
80
100
Transcriptional domain coverage (%)

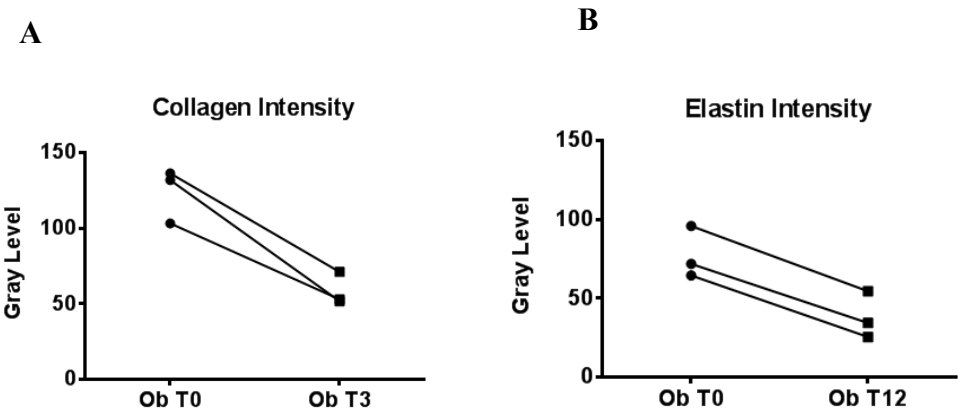
A
Collagen Intensity
150
100
50
0
Gray Level
Ob T0
Ob T3
B
Elastin Intensity
150
100
50
0
Gray Level
Ob T0
Ob T12

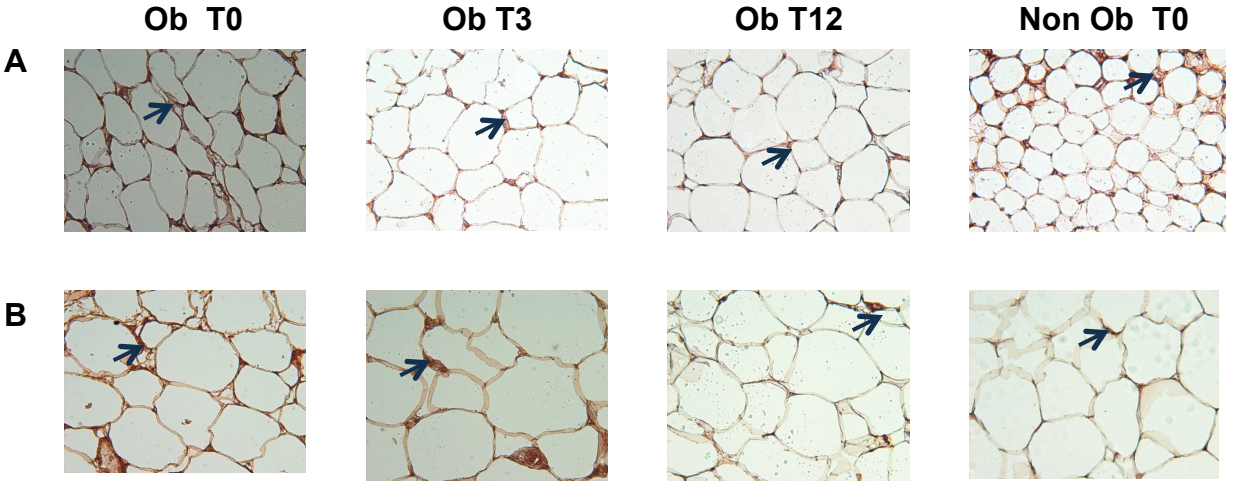
Ob T0
Ob T3
Ob T12
Non Ob T0
A
B